


RESEARCH

Open Access



Fetal echocardiography changes of the right ventricle of well-controlled gestational diabetes mellitus

Ying Ma¹, XueSong Sun², XiaoZhi Liu², LiHua Hu¹, Ye Song¹ and Xiong Ye^{3*} 

Abstract

Background There is few evidence of right ventricular (RV) function in fetuses with gestational diabetes mellitus (GDM). Therefore, the aim of this study was to assess the RV function of fetuses using routine and two-dimensional speckle-tracking echocardiography (2D STE) to determine the effects of well-controlled GDM in the third trimester.

Methods We used a Philips Epiq7C ultrasound instrument to obtain RV data sets from 63 subjects from July 2019 to February 2022. We compared the free wall thickness (FWT), fractional area change (FAC), Tei index (TEI), tricuspid annular plane systolic excursion (TAPSE) and free wall longitudinal strain(FWLS)of the RV in mothers with well-controlled GDM and normal gestational age-matched fetuses.

Results 63 third trimester fetuses (32 GDM; 31 healthy controls) met the enrolment criteria. Significant differences in fetal RV were detected between the GDM and control groups for the FAC (36.35 ± 6.19 vs. 41.59 ± 9.11 ; $P=0.008$) and the FWLS (-18.28 ± 4.23 vs. -20.98 ± 5.49 ; $P=0.021$). There was a significant difference among the segmental strains of the base, middle and apex of the RV free wall in the healthy controls ($P=0.003$), but in the GDM group, there was no statistical difference ($p=0.076$). RV FWLS had a strong correlation with FAC ($r=0.467$; $P=0.0002$).

Conclusions In well-controlled GDM, there was measurable fetal RV hypertrophy and significant systolic function decline, indicating the presence of ventricular remodeling and dysfunction. 2D-STE can evaluate the RV free wall contraction in a more comprehensive way.

Keywords Fetal echocardiography, Gestational diabetes mellitus, Right ventricle, Speckle tracking, Strain

Introduction

Gestational diabetes mellitus (GDM) is defined as any degree of glucose intolerance, onset or first detected during pregnancy [1], with a prevalence of 9–25% of all pregnancies worldwide in the last decade [2]. The prevalence of GDM in China is approximately 14.8% [3]. GDM is associated with adverse neonatal outcomes, including the risk of developing myocardial dysfunction and neonatal morbidity, even in good glycemic control [4]. Despite good glycemic control, 30% of diabetic mothers can cause fetal hypertrophic cardiomyopathy, sometimes leading to sudden intrauterine fetal death [5, 6]. Echocardiography

*Correspondence:

Xiong Ye

yex@sumhs.edu.cn

¹Department of Ultrasound, Zhou Pu Hospital, Shanghai University of Medicine & Health Sciences, Shanghai, China

²Department of Obstetrics and Gynecology, Zhou Pu Hospital, Shanghai University of Medicine & Health Sciences, Shanghai, China

³School of Clinical Medicine, Shanghai University of Medicine & Health Sciences, Shanghai, China



© The Author(s) 2023. **Open Access** This article is licensed under a Creative Commons Attribution 4.0 International License, which permits use, sharing, adaptation, distribution and reproduction in any medium or format, as long as you give appropriate credit to the original author(s) and the source, provide a link to the Creative Commons licence, and indicate if changes were made. The images or other third party material in this article are included in the article's Creative Commons licence, unless indicated otherwise in a credit line to the material. If material is not included in the article's Creative Commons licence and your intended use is not permitted by statutory regulation or exceeds the permitted use, you will need to obtain permission directly from the copyright holder. To view a copy of this licence, visit <http://creativecommons.org/licenses/by/4.0/>. The Creative Commons Public Domain Dedication waiver (<http://creativecommons.org/publicdomain/zero/1.0/>) applies to the data made available in this article, unless otherwise stated in a credit line to the data.

is a noninvasive screening tool for the assessment of cardiac structure and function of fetuses. The review of Depla's showed that presentational or gestational maternal diabetes is associated with fetal cardiac hypertrophy, diastolic dysfunction and impaired global myocardial function on obstetric ultrasonography [4].

There is little evidence currently available to estimate right myocardial damage that especially occurs in GDM. The fetal central circulation is a very flexible and adaptable circulatory system which differs from adults [7, 8]. At 28 to 32 weeks, the venous duct and foramen ovale shunt flow reached the minimum, and the partial lung flow reached the maximum [9]. The right heart occupies the advantage position of fetal circulation, right cardiac output accounts for 60 to 70% of total output, and the RV forms a greater proportion of the total ventricular weight than it does in childhood or adulthood [10]. Under these physiological baselines, the hemodynamic properties and functional range of these shunts are important determinants of fetal cardiac and circulatory development in the second and third trimesters [11].

Two-dimensional speckle tracking echocardiography (2D STE) is an imaging algorithm for changes in cardiac function [12, 13]. 2D STE has no dependence on ultrasound beam angulation and relatively small operator dependence [13]. Strain parameters are better than ejection fraction and have allowed detection of preclinical myocardial dysfunction [14]. It was found that the change in fetal myocardial strain occurred earlier than the traditional ultrasonic estimate of cardiac function [15, 16].

In this study, we aimed to explore the echocardiography changes of systolic function of fetal RV using traditional and 2D STE in well-controlled GDM mothers.

Materials and methods

Subjects

This prospective observational cross-sectional study included 32 fetuses (35.78 ± 0.790 weeks) of mothers with GDM as the case group and another 31 gestational age-matched fetuses (36.42 weeks ± 0.773) of normal pregnancies as the control group. Cases and controls were recruited from July 2019 to February 2022 at the Department of Ultrasound, Zhou Pu Hospital Affiliated to Shanghai University of Medicine & Health Sciences. Maternal medical records were reviewed in all subjects, including body mass index (BMI) and blood pressure.

Inclusion and exclusion criteria

Inclusion criteria: The cases were as follows: mothers aged 18 years or older with GDM as per the International Association of Diabetes and Pregnancy Study Group criteria [1] in the third trimester at Zhou Pu Hospital. The control group was normal pregnancies matched by gestational age. All the mothers with GDM only through

diet to controlled their blood glucose (fasting blood glucose < 5.3 mmol/L), and did not use oral hypoglycemic drugs or injected insulin.

The exclusion criteria were as follows: (1) fetal structural heart disease; (2) twin or multiple pregnancies; (3) pregnant women with hypertensive syndrome during pregnancy, hyperhydramnios, chronic kidney disease, liver disease, rheumatic disease, thyroid disease, autoimmune disease, etc.; (4) The anterior chest wall of the fetus does not face to or the placenta is located in the anterior wall of the uterus, and the distance of the fetus is far from the abdominal wall of the mother. (The fetal heart structure will cannot be clearly showed, and it is difficult to obtain a standard section to fit for measuring the cardiac function of the fetus.)

Equipment and ultrasonic image acquisition

Equipment A Philips Epiq7C color Doppler ultrasound diagnostic instrument (Philips Healthcare, Andover, MA) was adopted with c5-1 (5–10 MHz) probes. It was equipped with an offline Q-Lab 13.0 ultrasonic image workstation that has special software for right ventricular automatic strain quantitative analysis.

Ultrasonic image acquisition: Echocardiograms were performed at a single clinical site. All ultrasonic operations followed published guidelines for fetal echocardiography [17]. Image acquisition adjustments, such as sector width, depth, gain, focus or function of frequency and tissue harmonic, were used to optimize the frame rate (> 80 frames/sect.) [18]. A dynamic image dataset of 2 to 4 s was captured in the following views: 4-chamber view of the apical or basal fetal cross-section. Two experienced echo cardiographers (Ying Ma and LiHua Hu) performed the fetal echocardiography. All parameters were measured 3 times, and the average value was taken for analysis. Patients' diagnosis was blinded to operators at the time of the ultrasound image acquisition and offline analysis.

Fetal echocardiography

Conventional two-dimensional doppler fetal echocardiography (Fig. 1)

1) Right ventricular free wall thickness (RV FWT): M-mode was obtained perpendicular to the RV long axis in a 4-chambered view of the fetal heart to assess the RV FWT (Fig. 1a);

2) Tricuspid annular plane systolic excursion (TAPSE): The motion spectrum of the tricuspid annulus was measured by M-mode. According to the size of the heart, let the sampling line be consistent with the movement direction of the long axis of the RV at an angle of $< 20^\circ$, place the sampling line at the junction of the anterior tricuspid valve ring and the RV free wall, and obtain the motion spectrum of the tricuspid valve ring. TAPSE is the

longitudinal displacement of the tricuspid annulus from end systolic to end diastolic measured on the obtained tricuspid annulus motion curve (Fig. 1b);

3) Right ventricular fractional area changes (RV FAC): The edges of the RV at the end diastolic and end systolic endocardium were recorded. $RV\ FAC = (end-diastolic\ area - end-systolic\ area) / end-diastolic\ area \times 100\%$ (Fig. 1c);

4) Right ventricular Tei index (RV TEI): In the fetal 4-chamber view, the tissue Doppler sampling gate was placed on the lateral ring of the tricuspid valve to obtain the Doppler spectrum and calculate the RV TEI index. The RV TEI index is calculated by measuring time intervals including isovolumic contraction time (ICT) from tricuspid valve closure to pulmonic valve opening;

isovolumic relaxation time (IRT) from pulmonic valve closing to tricuspid valve opening; and ejection time (ET) from pulmonic valve opening to closing. $RV\ TEI = (ICT + IRT) / ET$, as described previously [19] (Fig. 1d).

Two-dimensional ultrasound speckle tracking technique

RV ultrasound images of fetal 4-chamber hearts were collected as two-dimensional gray scale images within three to four consecutive cardiac cycles. All images were analyzed by Q-Lab offline software using DICOM data without any loss of frame rate. From the 4-chamber apical view, the software automatically delineated the endocardial boundary of the RV and manually fine-tuned the systolic and diastolic boundaries to track the whole RV. The analysis software automatically divided the free wall

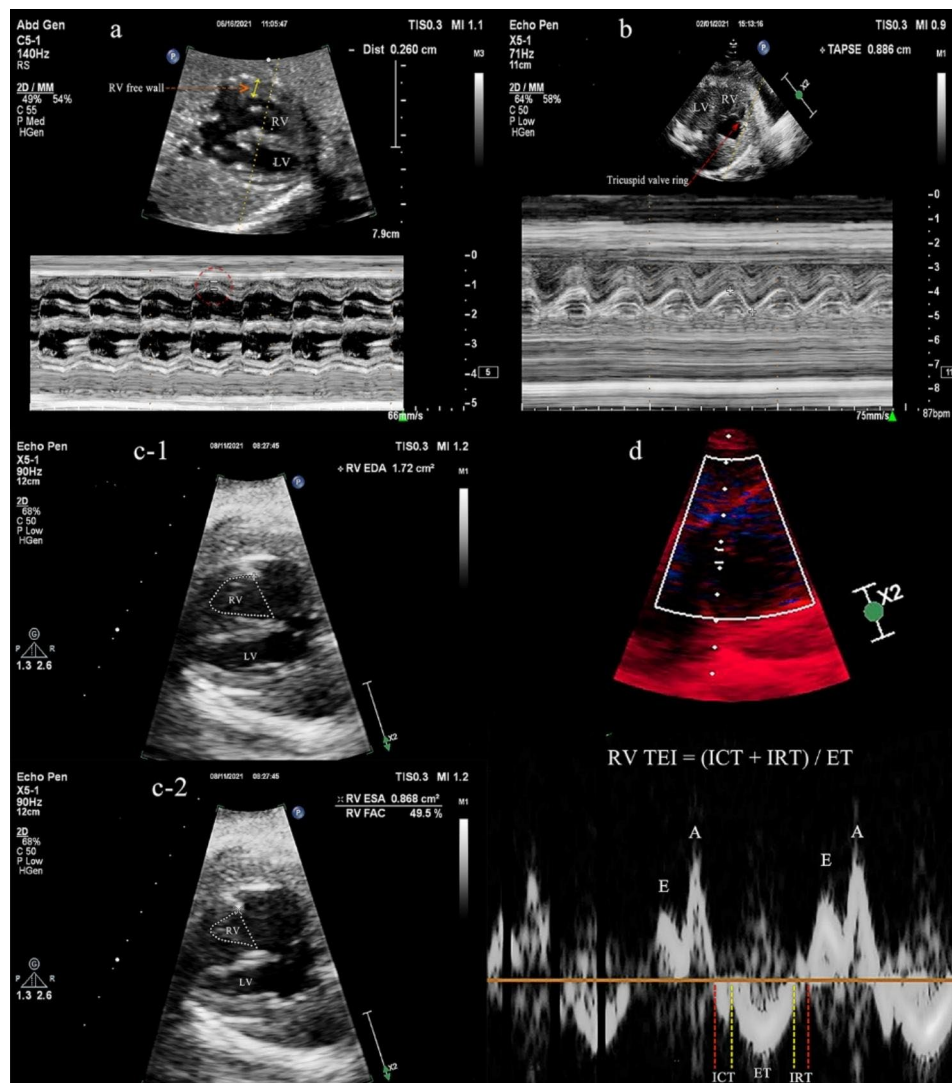


Fig. 1 Conventional fetal echocardiography (a) Right ventricular free wall thickness; (b) Tricuspid annular plane systolic excursion, longitudinal displacement of the tricuspid annulus from end systolic to end diastolic measured on the obtained tricuspid annulus motion curve; c-1-2. Right ventricular fractional area changes, (end-diastolic area - end-systolic area)/end-diastolic area $\times 100\%$; d. Right ventricular Tei index ($RV\ TEI = (ICT + IRT) / ET$), ICT, isovolumic contraction time; IRT, isovolumetric relaxation time; ET, ejection time)

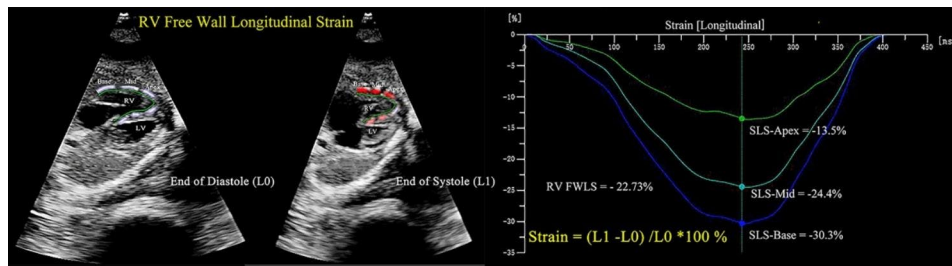


Fig. 2 Offline analysis of fetal right ventricular free wall segmental and integral longitudinal strains using Q-Lab 13.0. The initial length (L0) of the end diastolic of the three segments is shown on the left, and the length of the end systole (L1) is shown on the right

Table 1 Basic characteristic of pregnant women and fetuses (mean \pm SD)

Variables	Control group (N = 31)	GDM group (N = 32)	P values
Maternal characteristics			
Maternal age (years)	27.11 \pm 4.15	28.45 \pm 3.78	0.320
FBG (mmol/L)	4.78 \pm 0.78	6.37 \pm 1.61	< 0.0001
HbA1c (%)		5.60 \pm 0.20	
BMI (cm/s)	26.28 \pm 2.50	27.53 \pm 4.62	0.073
Systolic pressure (mmHg)	113.80 \pm 1.77	122.40 \pm 1.98	0.003
Diastolic pressure (mmHg)	63.89 \pm 1.24	68.11 \pm 1.76	0.060
Fetal characteristics			
Gestational age (wk.)	35.78 \pm 0.79	36.42 \pm 0.77	0.327
Fetal heart rate (beats/min)	146.60 \pm 9.37	146.00 \pm 8.51	0.776

BMI: body mass index; FBG: fasting blood glucose; GDM: gestational diabetes mellitus; HbA1c, glycated hemoglobin

of the RV into three equal-sized sections (basal, middle, and apical), tracking longitudinal strain in the region of interest (ROI). Longitudinal strain (LS) of the basal, middle and apical segments of the RV free wall is defined as the relative shortening of an ROI between the entire endocardial contour length at the end of diastole (L0) and end of systole (L1) ($LS = (L1 - L0) / L0 \times 100\%$) and by convention is expressed as a negative percentage [20]. The peak systolic RV free wall longitudinal strain (FWLS) was calculated as the average of the basal, mid, and apical RV free walls (Fig. 2).

Data analysis

We used SPSS version 25 (SPSS Inc., 2016, Armonk, NY) for all analyses. All variables were tested for normality before data were presented as either the mean \pm standard deviation (SD) or error of mean (SE), as appropriate. Differences between the two groups were compared using unpaired t-tests, and three groups were subjected to analysis of variance (one-way ANOVA) according to data characteristics. Correlation was tested by Pearson's correlation coefficient. P value < 0.05 was considered dominant.

Results

Characteristics of participants

Background characteristics are shown in Table 1. A total of 63 subjects were included for final analyses,

and 31 maternal controls were aged 27.11 \pm 4.15 years and 32 GDM cases aged 28.45 \pm 3.78 years ($p = 0.320$). The mean \pm SD of fasting blood glucose was 6.37 \pm 1.61 mmol/L and HbA1c was 5.60% (range, 5.40–5.80%) in the GDM group when they be diagnosed. There was no significant difference in mother's BMI, gestational age or fetal heart rate between the groups.

Parameters of fetal echocardiography

The results of the 2D conventional fetal heart ultrasound examination and 2D-STE analyses are provided in Table 2. Fetal RV FWT, TEI and TAPSE were not different, but the RV FAC and FWLS were significantly less in the GDM group than in the control group ($P = 0.008$; $P = 0.021$, respectively). There was a significant difference among the segmental strains of the base, middle and apex of the RV free wall in the healthy control group, but in the GDM group, there was no statistically significant difference (Fig. 3).

As shown in Table 3, when including all subjects (both healthy control and GDM groups), according to Pearson correlation analysis, we found that RV FWLS had a strong correlation with FAC ($r = 0.467$; $P = 0.0002$); gestational age was not correlated with RV TEI, FWT, TAPSE, FAC or FWLS.

Table 2 Fetal right ventricular changes in the control and GDM groups (mean ± SE)

Variables	Control group (n=31)	GDM group (n=32)	P values
FWT(mm)	2.41 ± 0.13	2.54 ± 0.09	0.460
TEI	0.45 ± 0.02	0.50 ± 0.02	0.054
FAC(%)	41.59 ± 1.82	36.35 ± 1.09	0.008
TAPSE(mm)	7.98 ± 1.07	7.84 ± 1.53	0.684
SLS-Base	-24.23 ± 8.28	-10.98 ± 18.90	0.001
SLS-Mid	-10.67 ± 1.49	-9.99 ± 3.34	0.306
SLS-Apex	-9.79 ± 3.42	-9.18 ± 2.71	0.380
FWLS	-20.98 ± 1.03	-18.28 ± 0.75	0.021

FWT: free wall thickness; FAC: fractional area change; FWLS: free wall longitudinal strain; GDM: gestational diabetes mellitus; TAPSE: tricuspid annular plane systolic excursion; TEI: Tei index; SLS-Apex: segmental longitudinal strain of apical; SLS-Base: segmental longitudinal strain of base; SLS-Mid: segmental longitudinal strain of middle

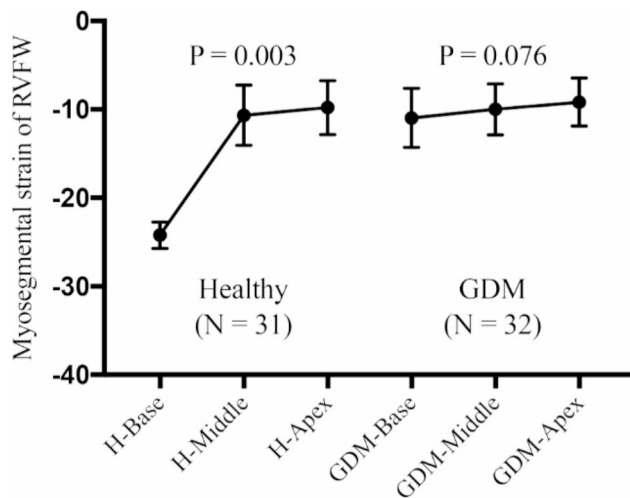


Fig. 3 Comparison of strains in each myocardial segment of the fetal right ventricular free wall in healthy pregnant women and GDM mothers

Intra-observer and inter-observer reproducibility

The reproducibility of RV overall and segmental free wall longitudinal strains was assessed in a subgroup of 15 randomly chosen subjects. Interclass correlation coefficients were moderate for both intra-observer and inter-observer analyses (Table 4).

Table 4 Intra- and inter-observer agreements of parameters of fetal right myocardial deformation on 2D STE (95% CI)

Parameters	Intra-observer	Inter-observer
FWLS	0.81 (0.65–0.82)	0.95 (0.87–0.98)
SLS-Base	0.87 (0.76–0.95)	0.82(0.77–0.95)
SLS-Mid	0.82 (0.75–0.92)	0.88 (0.75–0.92)
SLS-Apex	0.81 (0.64–0.89)	0.87 (0.69–0.96)

FWLS: free wall longitudinal strain; SLS-Base: segmental longitudinal strain of basal. SLS-Mid: segmental longitudinal strain of middle; SLS-Apex: segmental longitudinal strain of apical

Discussion

Pregnancies affected by diabetes often result in abnormal fetal development, including altered growth and nutrient distribution as well as congenital malformations [21]. Mothers with GDM have increased insulin resistance that can lead to maternal hyperglycemia and increased glucose transport across the placenta, with resultant fetal hyperinsulinaemia, which increases the synthesis and deposition of fat and glycogen in myocardial cells [22]. Elevated HbA (1c) values during the 1st trimester were associated with fetal cardiovascular defects in offspring [23]. The pathophysiology of the effects of maternal diabetes on the fetal heart is multifactorial and not fully understood, including the hyperglycemic environment, activation of a series of cellular events, and changes in gene expression [24–26].

There are several interesting results in our study. First, compared with normal pregnant fetuses matched with gestational age, the RV FAC and FWLS decreased significantly (P=0.008; P=0.021). This indicates RV hypertrophy and dysfunction in the fetal heart of GDM fetuses. This predicted a decrease in myocardial contractility and elasticity in GDM fetuses. Fetal hyperinsulinemia and insulin-like growth factor-I promote cardiomyocyte hypertrophy, leading to decreased myocardial compliance and function [27–29]. Second, there were no significant differences in the longitudinal strains of the basal, middle and apical parts of the free wall of right ventricle in GDM fetuses (p=0.076), but the differences were significant in healthy fetuses in different segments (p=0.003). This result similar to other studies [30] suggest that GDM fetal myocardium has significant diffuse impairment of RV function. To our knowledge, no

Table 3 Correlation coefficients among study variables of fetal right ventricular echocardiography (n=63, r values)

Items	FWLS	FAC	TEI	FWT	TAPSE	Gestational age
FWLS	1					
FAC	0.467#	1				
TEI	-0.222	-0.163	1			
FWT	-0.258	0.008	-0.363*	1		
TAPSE	-0.010	0.045	-0.097	0.003	1	
Gestational age	-0.200	-0.110	0.032	-0.114	0.052	1

FAC fractional area change, FWT free wall thickness, TEI: Tei index, TAPSE tricuspid annular plane systolic excursion; FWLS: free wall longitudinal strain. #P=0.0002; *p=0.007

other study has demonstrated the presence or absence of abnormal echocardiographic patterns to define the segmental nature of RV dysfunction that accompanies GDM. The RV myocardium mainly consists of deep longitudinal fibres [31], which play a key role in global RV contracts. Peak global longitudinal strain remains the most reliable quantitative tool for assessing RV function in children [32].

Third, we found that RV FWLS had a strong positive correlation with the right heart remodeling parameter FAC if we included all the control and GDM groups. In our and Willruth A. M. et al.'s studies (150 healthy fetuses at between 13 and 39 weeks gestation) [30], the correlation between RV FWLS and gestational age did not reach significance. However, Giovanni DS' study showed that there was significant correlation between gestational age and average peak longitudinal strain ($r = -0.73$; $P < 0.001$) in 100 20–32-week-old normal fetuses [33]. Possible reasons for this heterogeneity may include the use of different ultrasound systems and speckle-tracking algorithms [34]. Our study adds to the evidence for altered fetal RV structure and contractions in GDM.

There are few limitations of our study. First, it is a single-center, cross-sectional study with a relatively small sample size and a very narrow range of fetal gestational age. Echocardiographic analysis of the fetal heart is relatively difficult due to its small size and unfavorable location in the uterine cavity. Second, we did not study diastolic function because the fetal heart rate was close to 150 beats per minute. The rapid heart rate significantly shortened the diastolic period, resulting in poor repeatability of ultrasonic diastolic function measurements. Third, we needed to use multiple acoustic windows to view the right heart precisely from different perspectives; an experienced sonographer was required to complete the parameter measurement. Automatic algorithms for measuring fetal RV function need to be further developed.

Conclusion

In this study, echocardiography of right ventricular systolic properties was altered in well-controlled GDM fetuses compared with normal gestational age. 2-D SE revealed global and regional differences of strain in RVFW in GDM fetuses. We found heterogeneity in RV dysfunction of GDM fetuses, with no differences among the base, middle and apical segments, this suggest occult diffuse RV myocardial dysfunction. The mechanism of hyperglycemia on fetal cardiac structure and function needs be reached at future, the effect after delivery requires further follow-up studies.

Abbreviations

FWT	Free Wall Thickness
FAC	Fractional Area Change

FWLS	Free Wall Longitudinal Strain
GDM	Gestational Diabetes Mellitus
RV	Right Ventricular
2D STE	Two-dimensional Speckle-Tracking Echocardiography
TEI	Tei index
TAPSE	Tricuspid Annulus Plane Systolic Excursion
ICT	Isovolumetric Contraction Time
IRT	Isovolumetric Relaxation Time
ET	Ejection Time

Acknowledgements

This research was extracted from the Zhou Pu Hospital Affiliated to Shanghai University of Medicine & Health Sciences. We sincerely thank all the participants.

Authors' contributions

XY and YM contributed to the design of the study. YM and H LH contributed to obtaining the ultrasound images. S XS, L XZ, and SY were responsible for study subject recruitment and clinical data collection. XY contributed to the analysis of the data, prepared figures, and drafted the manuscript. All authors reviewed the manuscript and agreed to be accountable for all aspects of the work.

Funding

This work was supported by grants from the Pudong Municipal Health Commission of Shanghai (no. PW2021A-57), the Shanghai Municipal Health Commission (no. 201740227) and the Local High-Level University Construction Project (no. E1-2601-22-201006-5).

Data Availability

The datasets used and/or analyzed during the current study are available from the corresponding author on reasonable request. However, all data generated or analyzed during this study are included in this published article.

Declarations

Ethics approval and consent to participate

The study was conducted according to the requirements of the Declaration of Helsinki and approved by the Ethical Committee of Shanghai University of Medicine & Health Sciences (No: 2019-01-1267). Written informed consent was obtained from the participants for the publication of clinical details and ultrasonic images.

Consent for publication

Not applicable.

Competing interests

The authors declare that there is no conflict of interest.

Received: 30 January 2023 / Accepted: 27 September 2023

Published online: 06 October 2023

References

1. Metzger BE, Gabbe SG, Persson B, et al. International association of diabetes and pregnancy study groups recommendations on the diagnosis and classification of hyperglycemia in pregnancy. *Diabetes Care*. 2010;33(3):676–82.
2. Dalfrà MG, Burlina S, Del Vecovo GG, et al. Genetics and Epigenetics: New Insight on Gestational Diabetes Mellitus. *Front Endocrinol*. 2020;11:602477.
3. Gao C, Sun X, Lu L, et al. Prevalence of gestational diabetes mellitus in mainland China: a systematic review and meta-analysis. *J Diabetes Invest*. 2019;10(1):154–62.
4. Depla AL, De Wit L, Steenhuis TJ, et al. Effect of maternal diabetes on fetal heart function on echocardiography: systematic review and meta-analysis. *Ultrasound in Obstetrics & Gynecology*. 2021;57(4):539–50.
5. Balsells M, Garcia-Patterson A, Gich I, et al. Major congenital malformations in women with gestational diabetes mellitus: a systematic review and meta-analysis. *Diab/Metab Res Rev*. 2012;28(3):252–7.
6. Dickens LT, Thomas CC. Updates in gestational diabetes prevalence, treatment, and Health Policy. *Curr Diab Rep*. 2019;19(6):33.

7. Kiserud T. Physiology of the fetal circulation. *Semin Fetal Neonatal Med.* 2005;10(6):493–503.
8. Morton SU, Brodsky D. Fetal physiology and the transition to Extrauterine Life. *Clin Perinatol.* 2016;43(3):395–407.
9. Kiserud T, Acharya G. The fetal circulation. *Prenat Diagn.* 2004;24(13):1049–59.
10. Hislop A, Reid L. Weight of the left and right ventricle of the heart during fetal life. *J Clin Pathol.* 1972;25(6):534–6.
11. Tan CMJ, Lewandowski AJ. The Transitional Heart: from early embryonic and fetal development to neonatal life. *Fetal Diagn Ther.* 2020;47(5):373–86.
12. Leitman M, Lysyansky P, Sidenko S, et al. Two-dimensional strain—a novel software for real-time quantitative echocardiographic assessment of myocardial function. *J Am Soc Echocardiogr.* 2004;17(10):1021–9.
13. Blessberger H, Binder T. NON-invasive imaging: two dimensional speckle tracking echocardiography: basic principles. *Heart.* 2010;96(9):716–22.
14. Geyer H, Caracciolo G, Abe H, et al. Assessment of myocardial mechanics using speckle tracking echocardiography: fundamentals and clinical applications. *J Am Soc Echocardiography: Official Publication Am Soc Echocardiography.* 2010;23(4):351–69. quiz 453 – 355.
15. Chelliah A, Dham N, Frank LH, et al. Myocardial strain can be measured from first trimester fetal echocardiography using velocity vector imaging. *Prenat Diagn.* 2016;36(5):483–8.
16. Lee-Tannock A, Hay K, Gooi A, et al. Global longitudinal reference ranges for fetal myocardial deformation in the second half of pregnancy. *J Clin Ultrasound: JCU.* 2020;48(7):396–404.
17. Satomi G. Guidelines for fetal echocardiography. *Pediatr Int.* 2015;57(1):1–21.
18. DeVore GR, Polanco B, Satou G, et al. Two-Dimensional Speckle Tracking of the fetal heart: a practical step-by-step Approach for the fetal sonologist. *J Ultrasound Medicin.* 2016;35(8):1765–81.
19. Tei C, Nishimura RA, Seward JB, et al. Noninvasive doppler-derived myocardial performance index: correlation with simultaneous measurements of cardiac catheterization measurements. *J Am Soc Echocardiograph.* 1997;10(2):169–78.
20. Marwick TH, Leano RL, Brown J, et al. Myocardial strain measurement with 2-dimensional speckle-tracking echocardiography: definition of normal range. *JACC Cardiovasc Imaging.* 2009;2(1):80–4.
21. Grev JE, Munger KM, Scott SM. Infant of a Diabetic Mother. *South Dak Med Clin.* 2020;73(7):323–7.
22. Gellis SS, Hsia DY. The infant of diabetic mother. *A M A Journal of Diseases of Children.* 1959;97(1):1–41.
23. Lisowski LA, Verheijen PM, Copel JA, et al. Congenital heart disease in pregnancies complicated by maternal diabetes mellitus. An international clinical collaboration, literature review, and meta-analysis. *Herz.* 2010;35(1):19–26.
24. Nolan CJ, Damm P, Prentki M. Type 2 diabetes across generations: from pathophysiology to prevention and management. *Lancet.* 2011;378(9786):169–81.
25. Basu M, Garg V. Maternal hyperglycemia and fetal cardiac development: clinical impact and underlying mechanisms. *Birth Defects Research.* 2018;110(20):1504–16.
26. Basu M, Zhu JY, LaHaye S et al. Epigenetic mechanisms underlying maternal diabetes-associated risk of congenital heart disease. *JCI insight* 2017;2(20).
27. Zielinsky P, Piccoli AL. Jr. Myocardial hypertrophy and dysfunction in maternal diabetes. *Early Hum Dev.* 2012;88(5):273–8.
28. Gonzalez AB, Young L, Doll JA, et al. Elevated neonatal insulin-like growth factor I is associated with fetal hypertrophic cardiomyopathy in diabetic women. *Am J Obstet Gynecol.* 2014;211(3):290e291–297.
29. Gordon EE, Reinking BE, Hu S, et al. Maternal hyperglycemia directly and rapidly induces cardiac septal overgrowth in fetal rats. *J Diabetes Res.* 2015;2015:479565.
30. Willruth AM, Geipel AK, Fimmers R, et al. Assessment of right ventricular global and regional longitudinal peak systolic strain, strain rate and velocity in healthy fetuses and impact of gestational age using a novel speckle/feature-tracking based algorithm. *Ultrasound in Obstetrics & Gynecology.* 2011;37(2):143–9.
31. Caivano D, Rishniw M, Biretoni F et al. Transverse right ventricle strain and strain rate assessed by 2-Dimensional Speckle Tracking Echocardiography in Dogs with Pulmonary Hypertension. *Veterinary Sci* 2020;7(1).
32. Levy PT, Sanchez Mejia AA, Machevsky A, et al. Normal ranges of right ventricular systolic and diastolic strain measures in children: a systematic review and meta-analysis. *J Am Soc Echocardiograph.* 2014;27(5):549–60. e543.
33. Di Salvo G, Russo MG, Paladini D, et al. Two-dimensional strain to assess regional left and right ventricular longitudinal function in 100 normal fetuses. *Eur J Echocardiography.* 2008;9(6):754–6.
34. Alsolai AA, Bligh LN, Greer RM, et al. Myocardial strain assessment using velocity vector imaging in normally grown fetuses at term. *Ultrasound in Obstetrics & Gynecology.* 2018;52(3):352–8.

Publisher's Note

Springer Nature remains neutral with regard to jurisdictional claims in published maps and institutional affiliations.